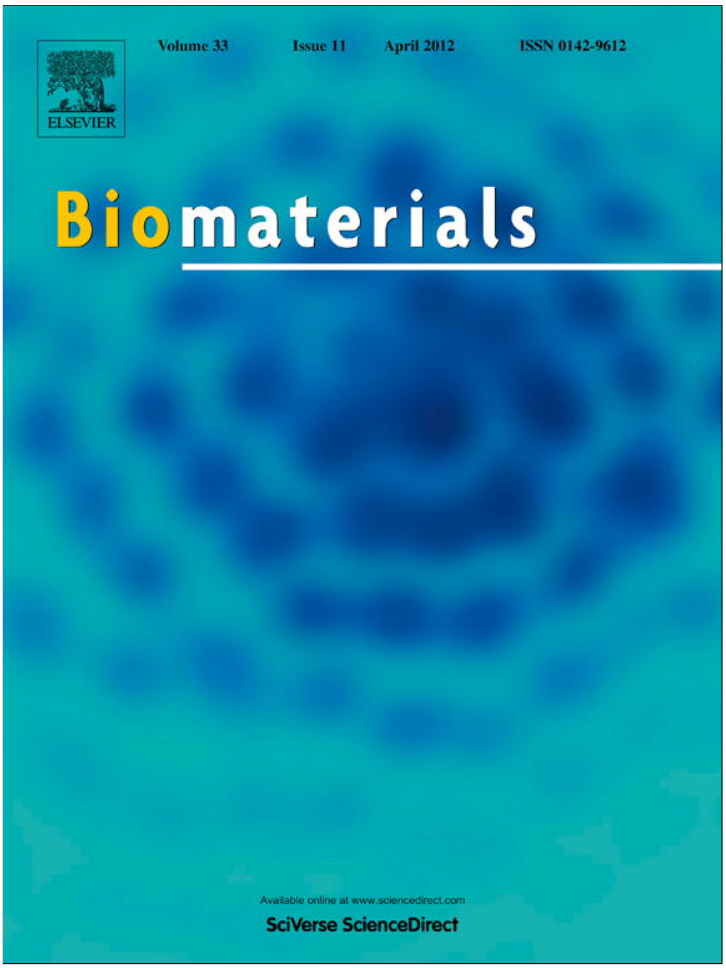

Biomaterials 33 (2012) 3235–3242

Contents lists available at SciVerse ScienceDirect

Biomaterials

journal homepage: www.elsevier.com/locate/biomaterials

Antitumor immunologically modified carbon nanotubes for photothermal therapy

Feifan Zhou [a,b], Shengnan Wu [a,b], Sheng Song [a,b], Wei R. Chen [a,c,**], Daniel E. Resasco [d], Da Xing [a,b,*]

[a] MOE Key Laboratory of Laser Life Science & Institute of Laser Life Science, College of Biophotonics, South China Normal University, Guangzhou 510631, China
[b] Joint Laboratory of Laser Oncology with Cancer Center of Sun Yat-sen University, South China Normal University, Guangzhou 510631, China
[c] Biomedical Engineering Program, Department of Engineering and Physics, College of Mathematics and Science, University of Central Oklahoma, Edmond, OK 73034, USA
[d] School of Chemical, Biological and Materials Engineering, University of Oklahoma, 100 E Boyd Street, Norman, OK 73019, USA

ARTICLE INFO

Article history:
Received 1 December 2011
Accepted 13 December 2011
Available online 31 January 2012

Keywords:
Carbon nanotubes
Antitumor response
Photothermal therapy
Immunological effects

ABSTRACT

An immunologically modified nanotube system was developed using an immunoadjuvant, glycated chitosan (GC), as surfactant of single-walled carbon nanotube (SWNTs). This SWNT-GC system not only retained both optical properties of SWNTs and immunological functions of GC, but also could enter cells due to the carrier properties of SWNTs. Cellular SWNTs induced thermal destruction of tumor cells when irradiated by a near-infrared laser and, at the same time, cellular GC could serve both as damage associated molecular pattern molecules (DAMPs) and pathogen associated molecular pattern molecules (PAMPs) to enhance the tumor immunogenicity and enhance the uptake and presentation of tumor antigens, leading to special antitumor response. Using this system and a 980 nm laser, we treated tumors, both *in vitro* and *in vivo*, and investigated the induced thermal and immunological effects. Laser + SWNT-GC afford a remarkable efficacy in suppressing tumor growth in animal cancer models, in many cases resulting in complete tumor regression and long-term survival. Mice successfully treated by Laser + SWNT-GC could establish resistance to tumor rechallenge. This system forms a multifunctional temporal-spatial continuum, which can synergize photothermal and immunological effects. The Laser + SWNT-GC could represent a promising treatment modality to induce systemic antitumor response through a local intervention, while minimizing the adverse side effects.

1. Introduction

Single-walled carbon nanotubes (SWNTs) have been applied in various biological systems [1]. One intrinsic property of SWNTs is their ability to cross cellular membranes without eliciting cytotoxicity [2], as a unique quasi one-dimensional material, have been explored as novel delivery vehicles for drugs [3], proteins [4], and so on. Another intrinsic property of SWNTs is their strong optical absorbance in the near-infrared (NIR) region [5,6]. It was reported that SWNTs could enhance thermal destruction of cells during NIR laser irradiation [6,7]. Now it has been developed for tumor targeting [8] and tumor subcellular targeting photothermal therapy during NIR laser irradiation [9,10].

For biological applications, SWNTs should be prepared in aqueous suspension; surfactants are needed for stable dispersion to avoid aggregation of nanotubes. The electronic structure of SWNTs is sensitive to changes in the surrounding electrostatic environment. For example, their optical response can be greatly changed by surface charge transfers or by adsorption of molecules [11]. Therefore, it is crucial to have a SWNTs solution with appropriate optical properties for biomedical applications.

Photothermal therapy can be effective for local cancer treatment due to the sensitivity of tumor cells to temperature elevation [12]. However, tumor recurrence is the biggest problem facing the current thermal therapy. Weak immunogenicity of tumors seriously affected cancer therapy effects. Therefore, increasing immunogenicity of tumors can enhance therapeutic effects of any treatment modality. One such approach is to combiner selective photothermal therapy and active immunological stimulation to enhance the host tumor-specific immune responses and laser immunotherapy was developed based on this principle for the treatment of metastatic cancers [13–15].

In this work, we designed a multifunctional SWNTs system, utilizing the absorption properties of the SWNTs during NIR region to destroy tumor cells, utilizing the transport properties of the

* Corresponding author. MOE Key Laboratory of Laser Life Science & Institute of Laser Life Science, College of Biophotonics, South China Normal University, Guangzhou 510631, China. Tel.: +86 20 85210089; fax: +86 20 85216052.
** Corresponding author. MOE Key Laboratory of Laser Life Science & Institute of Laser Life Science, College of Biophotonics, South China Normal University, Guangzhou 510631, China. Tel.: +86 405 974 5147; fax: +86 405 974 3812.
E-mail addresses: wchen@uco.edu (W.R. Chen), xingda@scnu.edu.cn (D. Xing).

0142-9612/$ – see front matter © 2011 Elsevier Ltd. All rights reserved.
doi:10.1016/j.biomaterials.2011.12.029

SWNTs carry immunostimulant into tumor cells to enhance the tumor immunogenicity. In this study, we investigate the antitumor effects of this immunologically modified nanotube system in the treatment of tumors both *in vitro* and *in vivo*.

2. Materials and methods

2.1. SWNT-GC solutions preparation

To prepare the SWNT-GC solution, pristine CoMoCAT SWNTs of 2.5–3 mg were mixed with 7 ml aqueous GC of different concentrations. To disperse the SWNTs, the mixture was sonicated for 30 min using a Cole–Parmer Ultrasonic Processor (CPX750) at 22% amplitude. This suspension of SWNTs was then centrifuged at 30,150 g for 30 min. The final concentration of SWNT in GC solution was determined by comparing its optical absorbance with that of a calibration SWNT solution of known concentration. The resonance ratio, a measure of the ability of a surfactant to suspend individual nanotubes, for an SWNT suspension in GC was also measured.

2.2. GC-FITC and SWNT-GC-FITC functionalization

FITC (13 mM, 50 μl) was dissolved in DMSO, and then mixed with 1 ml GC or SWNT-GC solutions. After incubating the mixture for overnight at room temperature, avoiding light exposure, the GC-FITC or SWNT-GC-FITC solutions were filtrated through 100 kDa filters (Millipore) to remove excess FITC.

2.3. Cell culture

Mouse mammary tumor cell line EMT6, and mouse macrophage cell line RAW264.7 were cultured in RPMI 1640 (GIBCO), supplemented with 15% fetal calf serum (FCS), penicillin (100 units/ml), and streptomycin (100 μg/ml) in 5% CO_2, 95% air at 37 °C in a humidified incubator.

2.4. Animal models

EMT6 cells (1×10^6) in a 100 μl solution were injected into the flank region of female Balb/c mice, aged 6–8 weeks. Animals were used in experiments 7–10 days after tumor cell inoculation, when the tumors reached a size of approximately 300 mm^3.

2.5. Laser treatment

For *in vitro* cell treatment, tumor cells (1×10^4 per well) in 24-well tissue culture plates were incubated with different combinations of SWNT and GC for 2 h, rinsed with PBS, and exposed to light at a fluence of 60–120 J/cm^2 (0.5–1 W/cm^2 for 2 min). The light source was a 980 nm semiconductor laser.

For *in vivo* tumor treatment, tumor-bearing mice were divided into eight different treatment groups (16–20 mice/group).A solution of 100 μl containing 5 mg/ml (25 mg/kg) GC or 0.2 mg/ml (1 mg/kg) SWNT or 0.2 mg–5 mg/ml (1 mg–25 mg/kg) SWNT-GC was directly injected into the center of each tumor, 2 h before irradiation with a 980 nm laser. The light was delivered to the tumor using a fiber optic delivery system. The power density at the treatment area, which encompassed the tumor and 0.5 cm of the surrounding skin, was 0.75 W/cm^2 for treatment duration of 10 min. During laser irradiation, mice were anesthetized with an intraperitoneal injection of pentobarbital sodium (i.p. 2%) and were restrained in a specially designed holder. After treatment, the mice were observed daily and the tumors were measured every other day for a period of 100 days.

2.6. Cell death assays

Cell Cytotoxicity *in vitro* was performed with a colorimetric tetrazolium salt-based assay, Cell Counting Kit-8 (CCK8, Dojindo Laboratories, Kumamoto, Japan), as described previously [10]. To detect photothermal cytotoxicity, tumor cells were irradiated by the 980 nm laser at a fluence of 60–120 J/cm^2 (0.5–1 W/cm^2 for 2 min) with or without incubation with SWNT-GC. OD450, the absorbance value at 450 nm, was read with a 96-well plate reader (INFINITE M200, Tecan, Switzerland), to determine the viability of the cells.

For TUNEL Staining analysis, mice from each treatment group were sacrificed 3 h after treatment. Individual tumors were fixed in 10% neutral buffered formalin, processed routinely into paraffin, sectioned at 5 microns, stained with TUNEL fluorescence dye (FITC, Genmed, Boston, MA, USA) and examined by fluorescence microscopy.

For cell death statistic analysis *in vivo*, the tumors were harvest 3 h after treatment and physically dissociated. Single cells in suspension were stained with Annexin-V-FITC and PI (Becton Dickinson, Mountain View, CA, USA), and analysised by FACScanto II flow cytometry (Becton Dickinson) with excitation at 488 nm. Fluorescent emission of FITC was measured at 515–545 nm and that of DNA-PI complexes at 564–606 nm. Compensation was used wherever necessary.

2.7. Macrophage phagocytosis

For *in vitro* study on the macrophage phagocytosis of different stimulated cells, the macrophages (1×10^5) were labeled with the red fluorescent cell linker PKH26 (Sigma), and cocultured with treated cells (5×10^5) which labeled with green fluorescent PKH67 cell linker (Sigma) in a 24-well plate in a total volume of 500 μl complete RPMI 1640 for 24 h, with or without HSP polyclonal antibody incubation. Phagocytosis was measured by flow cytometry.

2.8. Confocal microscopy for imaging analysis

Fluorescence emissions from FITC and DAF-FM was observed using a commercial laser scanning microscope (LSM 510/ConfoCor 2 META) combination system (Zeiss, Jena, Germany) equipped with a Plan-Neofluar 40×/1.3 NA Oil DIC objective. FITC and DAF-FM was excited at 488 nm with an Ar-Ion laser (reflected by a beam splitter HFT 488 nm), and the fluorescence emission was recorded through a 500–530 nm IR band-pass filter.

2.9. Detection of IFNγ

To detect IFNγ secretion by macrophages when stimulated by tumor cells after treatments, macrophages were incubated with treated tumor cells in 24-well tissue culture plates. After 24 h of incubation, the supernatants were collected for ELISA detection.

3. Results

3.1. Characterization of SWNT-GC

A stable SWNT-GC solution was obtained after the final centrifugation (Fig. 1). The NIR absorption spectra of SWNT-GC exhibit a strong band around 980 nm (Fig. 1B), which is typical for CoMoCAT samples. The SWNT-GC suspension remained stable after storage for more than six months at 4 °C (Fig. 1C).

To detect the effects of 980-nm optical excitation of SWNT-GC, we carried out a control experiment by radiating an aqueous solution of SWNT-GC under various concentrations with different laser dose. Irradiated with a 980 nm laser at 0.5–1 W/cm^2 for 120 s, SWNT-GC solution (100 μg/ml) caused temperature increase about 30–60 °C, depended on the laser dose (Fig. S1A). Fig.S1B shows that the temperature increase was also depended on the concentration of SWNT-GC.

Compared the absorption spectra of SWNTs dissolved in GC to dissolved in PL-PEG, we found that SWNT-GC solution has more narrow and intense absorption band around 980 nm than SWNT-PEG solution (Fig. S1C). To compare the photothermal transfer efficiency, irradiated with a 980 nm laser at 0.75 W/cm^2 for 120 s, SWNT-GC solution (100 μg/ml) caused temperature increase by 50 °C, SWNT-PEG solution (100 μg/ml) caused temperature increase by 35 °C (Figs. S1D and E). These findings clearly demonstrated the higher enhanced absorption of the 980 nm light by the SWNT-GC.

To study the macrophage activation triggered by SWNT-GC, intracellular NO generation were analyzed. Macrophages were stained by DAF-FM DA to fluorescently label NO, and detected by confocal microscopy or flow cytometry after treatments. As shown in Fig. 2A and S2A, 4 h after treatment, the cells revealed a dramatic increase of DAF-FM fluorescence emission in GC or SWNT-GC-treated cell compared with a slow increase in SWNT-PEG treated cells, cells stimulated with LPS as positive controls. To further determine the SWNT-GC stimulation, we observed CD80 expression on dendritic cells with FACS (Fig. S2B). The results indicate that SWNT-GC as well as GC could stimulate NO production in macrophages (Fig. 2A), and also stimulated a similar level of CD80 expression, which indicated the maturation of dendritic cells (Fig. S2B).

Before SWNT-GC application in biological systems, the cytotoxicity on cells was analyzed. We selected four typical normal cell line (3T3, HUVEC) and tumor cell line (EMT6, MCF7), incubated with GC or SWNT-GC for 48 h, and detected the cell viability. The

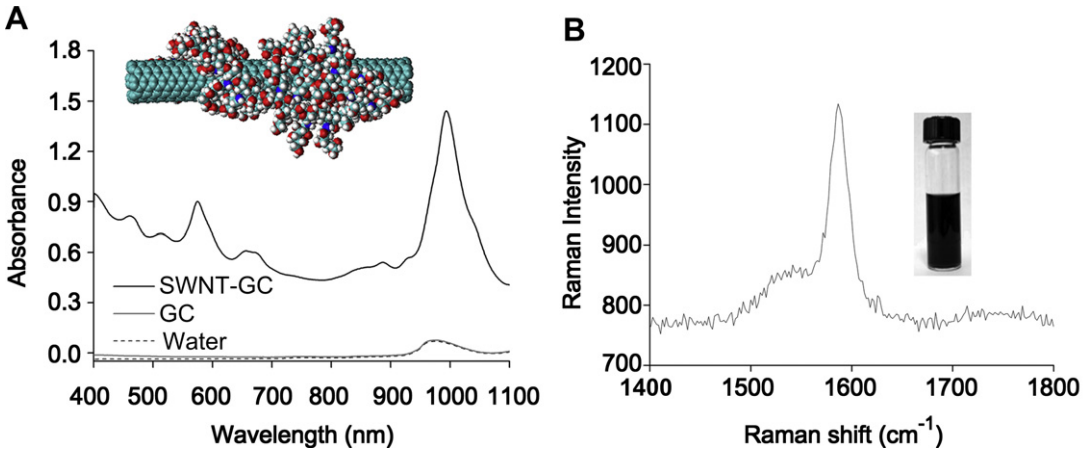

Fig 1. Optical characterization of the SWNT-GC system. A. Absorption spectra of SWNT-GC solution (200 μg–5 mg/ml) and GC solution (5 mg/ml). (Inset) Schematic of SWNT-GC interaction. B. Raman spectra of SWNT-GC. (Inset) A photo of a stable SWNT-GC suspension, after storage at 4 °C for more than six months.

results show that there was no obvious cytotoxicity on normal cells or tumor cells (Fig. S2C).

To confirm whether SWNT-GC could enter into tumor cells, we functionalized the SWNT-GC with FITC, a fluorescent tag, and observed the emission fluorescence from the tumor cell incubated with SWNT-GC-FITC or GC-FITC. Confocal images of the EMT6 cells show that SWNT-GC-FITC accumulates mainly in the cytoplasm, while GC-FITC are absent inside the cells (Fig. 2C). However, either SWNT-GC-FITC or GC-FITC could accumulate in RAW264.7 cells, because of the phagocytose property of macrophages.

These results indicate that GC can be used as efficient surfactants to obtain highly stable SWNT-GC suspensions, which not only retain the photothermal transducer properties of SWNT but also keep the immunological stimulation properties of GC. More importantly, as a unique quasi one-dimensional material, SWNT can carry GC into tumor cells.

3.2. Cooperative of SWNT-GC under laser irradiation in vitro

To determine the cytotoxicity of SWNT-GC under laser irradiation, EMT6 tumor cells were incubated with the SWNT-GC solution for 2 h, followed by irradiation with a 980 nm laser. Tumor cytotoxicity depended on both the SWNT-GC concentration and the laser dose (Fig. 3A).

To investigate the difference of the immune stimulation with treatments, we detected the HSP70 expression of treated tumor cells, which could be treated as the endogenesis danger signals to antigen-presenting cell (APC). Laser + SWNT-GC induced similar HSP70 expression level in the tumor cells (Fig. S3A), and resulted in similar count of surface HSP70-positive cells to Laser + SWNT-PEG (Fig. 3B and S3B).

ELISA was performed to measure IFNγ secreted by macrophages incubated with tumor cells after different treatments for 24 h. As

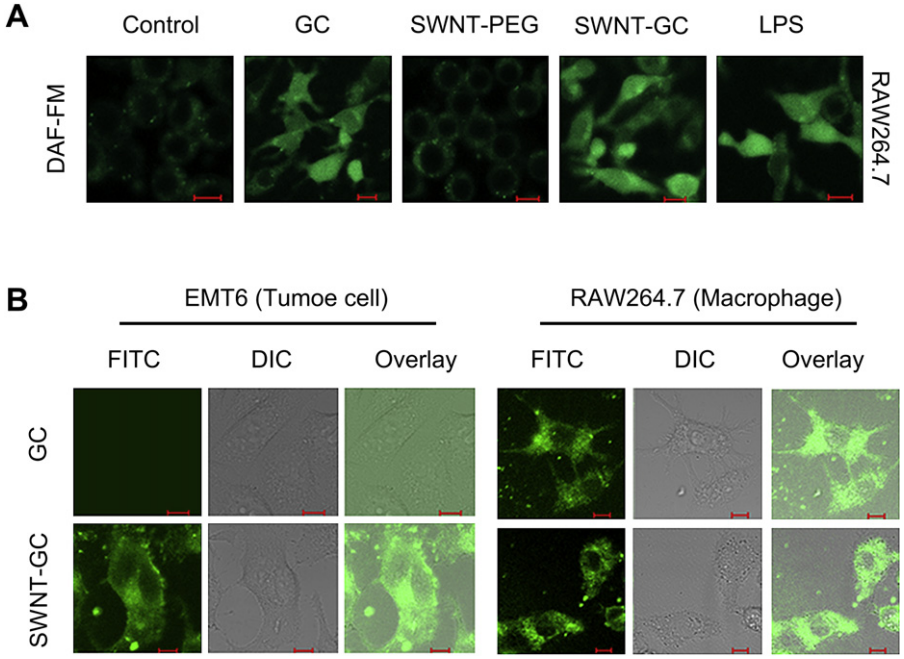

Fig. 2. Immunological functions of SWNT-GC. A. Fluorescent images of DAF-FM in macrophages. The macrophages were stimulated with different treatments, then stained with NO-sensitive fluorescent probes DAF-FM DA and observed under confocal microscope. B. Fluorescent images of SWNT-GC-FITC and GC-FITC in EMT6 or RAW264.7 cells. Cells were incubated with SWNT-GC-FITC and GC-FITC for 2 h, and the fluorescence of FITC from cells was detected by confocal microscope. Note that GC can enter tumor cells only when conjugated with SWNTs. Bar = 10 μm. All the data are representative of three independent experiments.

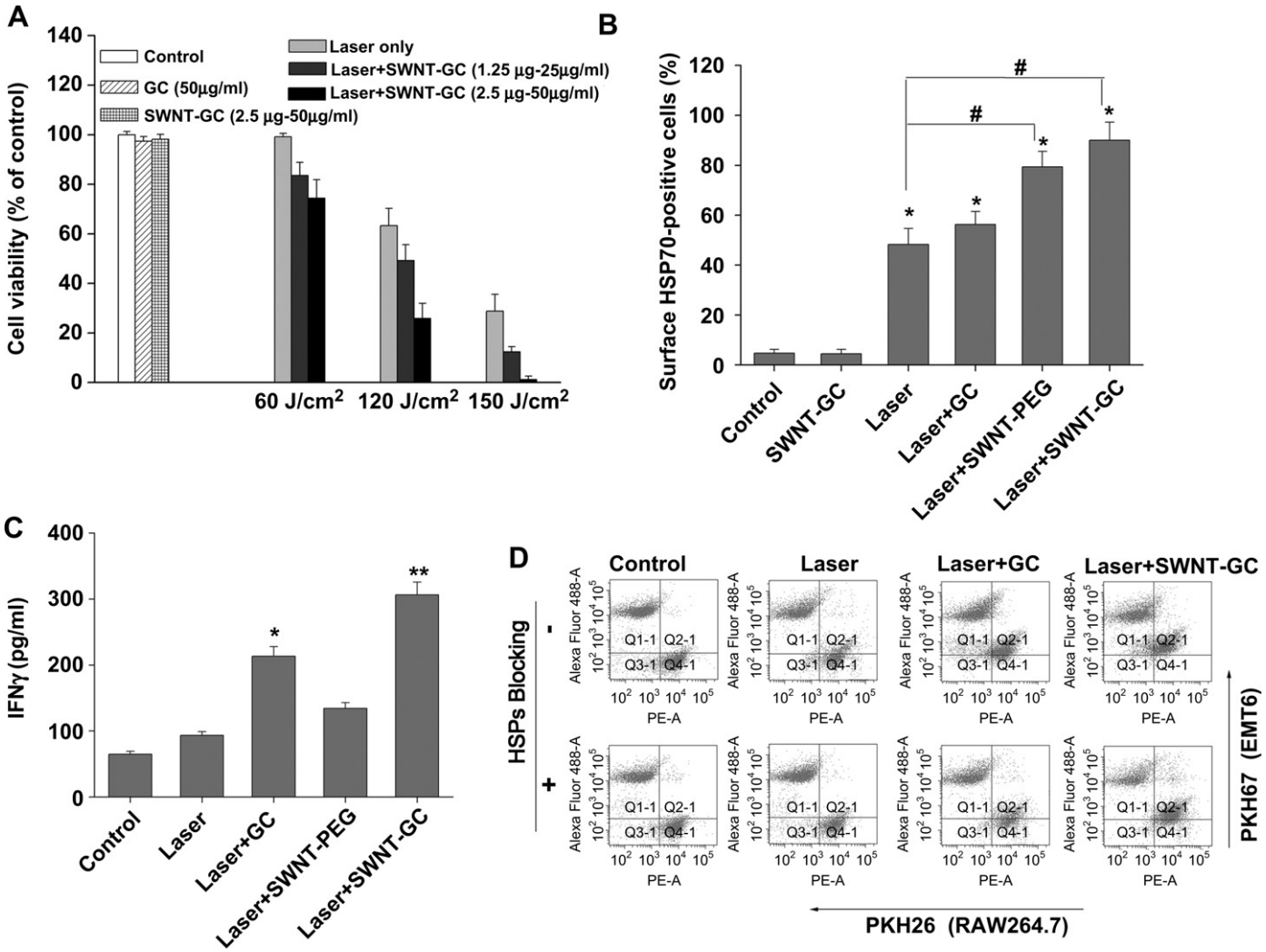

Fig. 3. *In vitro* cytotoxicity assays. A. Viability of tumor cells under different treatments. Tumor cells were treated with GC (50 μg/ml), SWNT-GC (2.5 μg–50 μg/ml), laser only (60–150 J/cm^2), or Laser + SWNT-GC (60–150 J/cm^2, 1.25 μg–25 μg/ml and 2.5 μg–50 μg/ml). The treated cells were incubated in complete medium for 12 h before assessing cell viability. Bars, means ± SD ($n = 6$). B. HSP70 detection on EMT6 cell surface 1 h after different treatments. Bars, means ± SD ($n = 6$), $^*P < 0.05$ *vs.* control cells; $\#P < 0.05$ *vs.* indicated cells. C. IFNγ secretion by macrophages stimulated by treated EMT6 cells. Macrophages were incubated for 24 h with treated tumor cells (1:5). Cells without treatment incubated with macrophages were used as control. After incubation, supernatants were collected for the determination of IFNγ by ELISA analysis. Bars, means ± SD ($n = 6$), $^*P < 0.05$; $^{**}P < 0.01$. D. Phagocytosis of tumor cells (vertical-axis) by macrophages (horizontal-axis) measured by FACS analysis. Macrophages (1×10^5 cells stained with PKH26, red) were incubated with treated tumor cells (5×10^5 cells stained with PKH67, green) for 24 h, with or without HSP polyclonal antibody incubation. The population of cells in the up-right quadrant of each group represents the interaction between treated tumor cells and macrophages. The data are representative of four independent experiments. Note that only in the Laser + SWNT-GC group (right column) blocking HSP does not affect the phagocytosis of tumor cells.

shown in Fig. 3C, tumor cells treated by laser or Laser + SWNT-PEG (120 J/cm^2) stimulated IFNγ secretion by macrophages, due to laser induced cell death (Fig. 3A). However, at these light doses, tumor cells treated by Laser + GC or Laser + SWNT-GC resulted in high levels of IFNγ secretion (Fig. 3C).

To explore how SWNT-GC stimulates a higher level of IFNγ secretion than SWNT-PEG under laser irradiation, even with similar endogenesis danger signals (HSP70 surface expression), we blocked the endogenesis danger signals with HSP polyclonal antibody and detected the phagocytose efficiency of macrophages incubated with treated tumor cells. The results show that except for the Laser + SWNT-GC group, phagocytosis efficiency is markedly decreased in the other treatment groups (Fig. 3D). We also observed that the SWNT-GC was exposed out of the tumor cells after laser treatment, and then was swallowed by macrophages under co-incubation (Fig. S3C). Furthermore, SWNT-GC could enhance the stimulation of dendritic cells with treated tumor cells, either for activation or phagocytosis of dendritic cells (Fig. S4).

These results indicate that SWNTs can enhance the tumor cytotoxicity under laser irradiation, due to the photothermal transducer properties, inducing the endogenesis of danger signals explosion. GC could enhance the stimulation of macrophages through treated tumor cells, acting as an immunologic adjuvant, either for macrophage activation or phagocytosis. The phagocytosis efficiency of macrophages depended on the endogenesis danger signals. However, the phagocytosis in the Laser + SWNT-GC group was independent of the endogenesis danger signals of tumor cells, as shown in Fig. 3D (far right). Because SWNT-GC can enter into the tumor cells, it should be considered as “endogenesis antigens” when tumor cell dies. Such “endogenesis antigens” induce the macrophage recognition even if endogenesis danger signals were blocked. Therefore, we clearly show the synergistic interaction of SWNT-GC between the selective photothermal reaction and

immunological stimulation, which enhances the cytotoxicity and immunogenicity of tumor cells, resulting in enhanced selective tumor cell destruction and antitumor immune response.

3.3. In vivo effects of SWNT-GC

First, the effects of SWNT-GC were evaluated using a mouse mammary tumor model. EMT6 cells were injected (s.c.) in the flank of Balb/c female mice. After the tumor size reached approximately 300 mm^3, the animals were divided into eight different treatment groups (16 mice per group). After treatment, the mice were observed daily and mice were determined when their tumor burden reached 8000 mm^3.

We investigated the photothermal effect of the SWNT-GC for selective destruction of the neoplastic tissue. Mouse tumor was injected with SWNT-GC (1 mg–25 mg/kg), and at 2 h post injection, the tumor was irradiated by the laser with a power density of 0.75 W $cm/^2$ for 10 min. The spot size of the laser beam was adjusted to cover the entire tumor (Fig. S5A, left). During the laser irradiation, full-body thermographic images were captured using an infrared camera (Fig. S5A, left). The temperature of the irradiated area was plotted as a function of the irradiation time (Fig. S5A, right). For the SWNT-GC-injected mice, the tumor surface temperature increased rapidly within 2 min to reach 62 °C and began to plateau after 5 min at 72 °C. In the case of un-injected mice, the surface temperature only increased to 47 °C.

To confirm tumor cytotoxicity of Laser + SWNT-GC treatment, scathe levels in the tumors were examined 3 h after treatment using TUNEL staining. The SWNT-GC-treated tumor showed similar scathe cells compared to the untreated tumor. In contrast, a high scathe level was observed in the cells treated by Laser + SWNT-GC or Laser + SWNT-PEG (Fig. 4A, upper panel). To determine tumor destruction by the photothermal treatment, single cells dissociated from treated tumors were analyzed by FACS. Laser only treatment induced 42.7% cell death, with typical necrosis characteristic; Laser + SWNT-GC or Laser + SWNT treatment induced 89.2% and 73.1% apoptosis, respectively (Fig. 4A lower panel and Fig. 4B).

For survival studies, mice were monitored for 100 days after tumor inoculation. Among mice treated by a single injection of SWNT-PEG (1 mg), GC (25 mg/kg), or SWNT-GC (1 mg–25 mg/kg) solution, there were no long-term survivors, although mice in GC and SWNT-GC groups had a slightly longer average survival time (Fig. S5B). Under laser irradiation at a power density of 0.75 W/cm^2, the survival rates were 100% in the Laser + SWNT-GC group, 43.75% in the Laser + SWNT-PEG group, 25% in the Laser + GC group, and 12.5% in the laser only group, respectively (Fig. 4C).

Mouse hepatoma tumor model (H22) was also used for survival studies. In the Laser + SWNT-GC group, the survival rates were 90% (Fig. S5C). All mice in other treatment groups developed primary tumors and died within 60 days (Fig. S5C).

At the conclusion of the survival studies, all the mice bearing EMT6 tumors in the Laser + SWNT-GC group were alive, with complete tumor regression. Six of the ten mice bearing H22 tumors in the Laser + SWNT-GC group survived with complete tumor regression (Fig. S5D).

Overall, our results demonstrated that Laser + SWNT-GC was the most efficacious treatment, resulting in a much higher survival rate and stronger tumor suppression than other combinations of laser, SWNT, and GC.

3.4. Long-term antitumor effects of Laser + SWNT-GC treatment

Mice successfully treated by Laser + SWNT-GC and Laser + SWNT-PEG were challenged with 2×10^6 viable EMT6 tumor cells 100 days after the initial tumor inoculation (10 mice per group). Ten mice of the same age were inoculated with 2×10^6 viable tumor cells per mouse as controls. As shown in Fig. 5A, all the Laser + SWNT-GC cured mice showed total resistance to the challenge. However, all the Laser + SWNT-PEG cured mice developed primary tumors and died within 80 days of tumor rechallenge. The Laser + SWNT-GC cured mice were challenged a second time with an increased tumor dose (3×10^6/mouse).

To study antitumor activity of SWNT-GC, EMT6 tumor cells were implanted on both right and left flanks of the mice. Only the tumor on the left side was treated while the tumor on the right side served as the observation point without treatment. Our results showed that the growth of the untreated left tumor was significantly inhibited when the tumor on the right side was treated with Laser + SWNT-GC. However, the left tumors were not impacted by the treatment of right tumors with Laser + SWNT-PEG (Fig. 5B).

In another experiment, we implanted EMT6 tumor cells only on the right flank of the mice. On the left flank, the mice received a topical application of SWNT-GC, followed by laser irradiation. Tumor growth on the right side of the mice was not affected by the Laser + SWNT-GC treatment on the left (Fig. S6). These results suggest that the application of SWNT-GC in a viable tumor is the prerequisite for the induction of effective antitumor immune responses.

To further study antitumor immune response of SWNT-GC, we compared the therapy efficacies of Laser + SWNT-GC in immunocompetent mice and immunodeficiency mice (thymic deletion), bearing EMT6 tumor. As shown in Fig. 5C, the survival rate of treated immunodeficiency mice was low, indicating that T cells are necessary for the induction of effective antitumor immune responses.

These results indicate that Laser + SWNT-GC treatment induces long-term special antitumor immune responses, mediated by T cells and depend on the presence of tumor antigens.

4. Discussion

Our experimental results clearly show that the SWNT-GC solution retained the optical properties of SWNTs (Fig. 1 and S1) and the immunological properties of GC (Fig. 2 and S2). The resonance ratio for the SWNT suspension in GC was measured to be 0.140, which favorably compares to NaCholate (with a similar ratio of 0.147), one of the best surfactants reported in literature [11]. We also found the absorption of SWNT-GC was higher that SWNT-PEG, which is a common surfactant for SWNTs (Fig. 1). More importantly, SWNT can carry GC into tumor cells, due to its transport function, as a unique quasi one-dimensional material (Fig. 2C), which fulfills a crucial step for temporally and spatially synchronized photo-immunological interaction under laser irradiation.

The advantage of the SWNT-GC system lies in its synergistic reactions during tumor treatment. Specifically, SWNTs selectively absorb the 980 nm laser light to induce the destruction of tumor cells. (Fig. 3A), hence providing an exogenous cellular stress and leading to the secretion of damage associated molecular pattern molecules (DAMPs) (Fig. 3B). DAMPs are intracellular molecules that are normally hidden within live cells, which acquire immunostimulatory properties upon exposure or secretion by damaged/dying cells. These molecules have the ability to exert various effects on antigen-presenting cells, such as maturation, activation and antigen processing/presentation [16]. DAMPs include intracellular proteins, such as heat-shock proteins or HMGB1 (high-mobility group box 1).

In addition, GC serves as a pathogen associated molecular pattern molecules (PAMPs) and can enhance phagocytose and

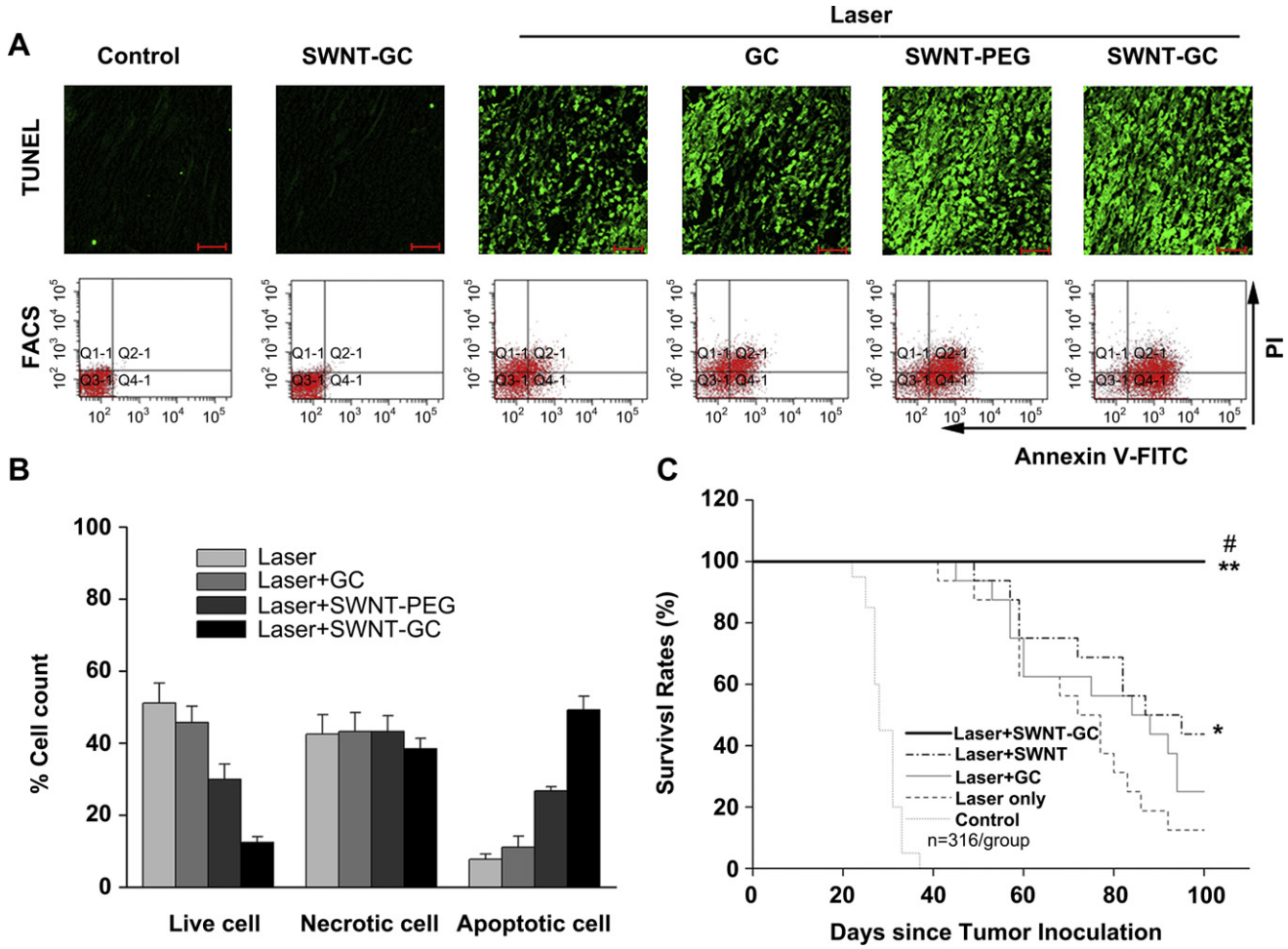

Fig. 4. *In vivo* cytotoxicity assays. EMT6 cells were injected (s.c.) in the flanks of Balb/c female mice, and treatment took place when tumors reached a size of approximately 300 mm^3. Tumors were treated with intratumoral injections of different components, followed by laser irradiation (0.75 W/cm^2 for 10 min): (i) Control, (ii) SWNT (1 mg/kg), (iii) GC (25 mg/kg), (iv) SWNT-GC (1 mg–25 mg/kg), (v) Laser only, (vi) Laser + SWNT (1 mg/kg), (vii) Laser + GC (25 mg/kg), (viii) Laser + SWNT-GC (1 mg–25 mg/kg). A. TUNEL staining and FACS analysis of the excised EMT6 tumors 3 h after different treatments: (i) Control, (iv) SWNT-GC, (v) Laser, (vii) Laser + GC, (vi) Laser + SWNT, or (viii) Laser + SWNT-GC. The upper images are TUNEL staining of representative specimens. Bar = 50 μm. The lower images are FACS analysis of single tumor cells dissociated from treated tumors, double stained by Annexin-V-FITC/PI and analyzed by FACS. High scathe level was observed in the Laser + SWNT-GC and Laser + SWNT treated tumors. The data are representative of four independent experiments. B. The quantified analysis of apoptotic and necrotic cells percentage according to C. Bars, means ± SD ($n = 4$). C. Survival rates of EMT6 tumor-bearing mice treated by intratumoral injections of different components followed by laser irradiation at 0.75 W/cm^2 for 10 min $^*P < 0.05$ *vs.* laser only group; $^{**}P < 0.0005$ *vs.* Laser only group; $\#P < 0.005$ *vs.* Laser + SWNT group (16 mice/group).

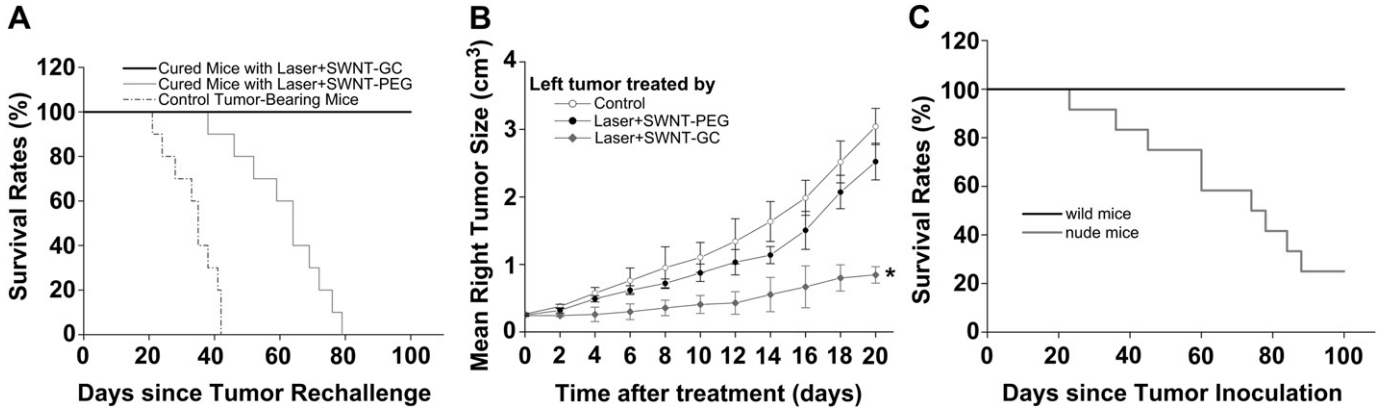

Fig. 5. Long-term antitumor effects. A. Tumor rechallenge of successfully treated mice. EMT6 tumor-bearing mice cured by Laser + SWNT-GC or Laser + SWNT treatment were challenged with 2×10^6 viable EMT6 tumor cells 100 days after the initial inoculation. Naive mice of the same age were also inoculated with 2×10^6 viable tumor cells as controls. Only the mice cured by Laser + SWNT-GC showed total resistance to the challenge. (10 mice/group). B. Systemic effect of Laser + SWNT-GC. Mice received EMT6 tumor cell injections on both left and right flanks. Tumors on the left side were treated with Laser + SWNT or Laser + SWNT-GC. Tumor size on the right side was measured every other day after treatment. Bars, means ± SD ($n = 10$), $^*P < 0.0005$ *vs.* control group. C. Survival rates of EMT6 tumor-bearing Balb/c wild type (immunocompetent) or Balb/c nude mice (thymic deletion) treated by Laser ± SWNT-GC (10 mice/group).

activation efficiency of macrophages (Fig. 3C and D). PAMPs are molecules associated with groups of pathogens that are recognized by cells of the innate immune system. They activate innate immune responses, protecting the host from infection, by identifying some conserved non-self molecules. In the SWNT-GC system, when GC is exposed, it serves both as PAMPs and DAMPs, which enhance the immunogenicity of tumors, increase the tumor antigen uptake by APCs (Fig. 3D and S4A), and enhance the activation of APCs (Fig. 3C and S4B).Therefore, because of the unique bound of SWNT and GC, they can target the same tumor cell at the same time. Firstly, SWNT selectively absorb laser light to induce tumor cell death. Secondly, the PAMPs (GC) carried into the tumor cells was exposed as DAMPs, to enhance the immunogenicity of tumors and induce APCs activations. Hence, the SWNT-GC act as a perfect temporal-spatial continuum, connect the tumoricidal and immune response process, resulting in a synergistic photothermal immunological reaction.

Intratumoral injection of SWNT-GC did not result in tumor regression (Fig. 4A), although prolonged the medium survival time of the mice (Fig. S5B). This result could be attributed to the nonspecific immune response of host, induced by GC. When laser irradiation was used, the therapeutic effect of SWNT-GC was significantly enhanced. Laser + SWNT-GC and Laser + SWNT-PEG treatment both induced much higher levels of tumor cell death, with significant apoptosis characteristic, compared with the lower level of tumor cell death induced by laser only treatment, with necrosis characteristic (Fig. 4A and B). On the one hand, the enhanced tumor-killing effect was due to the fact that SWNT can selectively absorb the 980 nm laser light. On the other hand, the high level apoptosis was due to thermal effect from the intracellular SWNT. However, Laser + SWNT-GC treatment achieved higher level of tumor cell death than Laser + SWNT-PEG treatment (89.2% versus 73.1%). It may be due to the fact that the GC molecules were difficult to be metabolized, hence retaining more SWNTs in the tumors. In addition, our previous study found that apoptotic cell can afford more tumor antigens and induce higher effect immune response than necrotic cells during photodynamic therapy [17].

The survival study demonstrated that with a laser power density of 0.75 W/cm^2 and irradiation duration of 10 min for both EMT6 and H22 tumor models, the presence of SWNT-GC resulted in significantly high survival rates (Fig. 4C and S5C and D). The resistance to tumor rechallengs by cured mice (Fig. 5A) indicates the essential role of SWNT-GC in inducing long-lasting antitumor immunity.

By treating one tumor on one side of the mice, the untreated tumor on the opposite side was clearly affected by the Laser + SWNT-GC. The results shown in Fig. 5B and Fig. S6 indicate that SWNT-GC inside a viable tumor is a prerequisite for the induction of effective antitumor immune response. The study using immunodeficiency mice (thymus deficient mice) indicates that T cell response is necessary for the induction of effective antitumor immune response (Fig. 5C).

Although further investigation is needed, we can hypothesize the mechanism of Laser + SWNT-GC in the treatment of tumors. It relies on the synergistic interaction between the selective photothermal reaction and immunological stimulation at the same site. During the treatment, the SWNT-GC act as a perfect temporal-spatial continuum and the photothermal reaction by SWNT reduces the tumor burden and at the same time exposes the tumor antigens and GC, which together induces T-cell immune responses. Each individual host, in fact, produced an *in situ* auto-vaccine after the treatment. This tandem effect not only resulted in total tumor eradication but also led to a long-term tumor-specific immunity.

5. Conclusion

An immunologically modified nanotube system was used to provide synergistic photothermal and immunological effects under laser irradiation for cancer treatment. This SWNT-GC system not only retained both optical properties of SWNT and immunological functions of GC, but also could enter cells due to the carrier properties of SWNT. Cellular SWNT induced thermal destruction of tumor cells when irradiated by a near-infrared laser and, at the same time, cellular GC could serve both as DAMPs and PAMPs to enhance the tumor immunogenicity and enhance the uptake and presentation of tumor antigens, leading to special antitumor response.

Author contributions

Feifan Zhou, Da Xing, Wei R. Chen conceived and designed the experiments.

Wei R. Chen and Daniel E. Resasco constructed the SWNT-GC system.

Feifan Zhou, Shengnan Wu, Sheng Song performed the experiments.

Feifan Zhou, Da Xing, and Wei R. Chen analyzed the data.

Feifan Zhou and Wei R. Chen prepared the manuscript.

Acknowledgments

This research is supported by the National Basic Research Program of China (2011CB910402; 2010CB732602), the Program for Changjiang Scholars and Innovative Research Team in University (IRT0829), and the National Natural Science Foundation of China (30870676; 81101741), Science and Technology Planning Project of Guangdong Province (2011B031300008), and by the US National Institutes of Health (P20 RR016478 from the INBRE Program of the National Center for Research Resources).

Appendix. Supplementary information

Supplementary information associated with this article can be found, in the online version, at doi:10.1016/j.biomaterials.2011.12.029.

References

[1] Kostarelos K, Bianco A, Prato M. Promises, facts and challenges for carbon nanotubes in imaging and therapeutics. Nat Nanotech 2009;4:627–33.
[2] Porter AE, Gass M, Muller K, Skepper JN, Midgley PA, Welland M. Direct imaging of single-walled carbon nanotubes in cells. Nat Nanotech 2007;2:713–7.
[3] Liu Z, Chen K, Davis C, Sherlock S, Cao Q, Chen X, et al. Drug delivery with carbon nanotubes for in vivo cancer treatment. Cancer Res 2008;68:6652–60.
[4] Kam NWS, Jessop TC, Wender PA, Dai H. Nanotube molecular transporters: internalization of carbon nanotube-protein conjugates into mammalian cells. J Am Chem Soc 2004;126:8650–1.
[5] O'Connell MJ, Bachilo SM, Huffman CB, Moore VC, Strano MS, Haroz EH, et al. Band gap fluorescence from individual single-walled carbon nanotubes. Science 2002;297:593–6.
[6] Kam NWS, O''Connell M, Wisdom JA, Dai H. Carbon nanotubes as multifunctional biological transporters and near-infrared agents for selective cancer cell destruction. Proc Natl Acad Sci USA 2005;102:11600–5.
[7] Moon HK, Lee SH, Choi HC. In vivo near-infrared mediated tumor destruction by photothermal effect of carbon nanotubes. ACS Nano 2009;3:3707–13.
[8] Zhou F, Xing D, Ou Z, Wu B, Resasco DE, Chen WR. Cancer photothermal therapy in the near-infrared region by using single-walled carbon nanotubes. J Biomed Opt 2009;14:021009.
[9] Zhou F, Xing D, Wu B, Wu S, Ou Z, Chen WR. New insights of transmembranal mechanism and subcellular localization of non covalently modified single-walled carbon nanotubes. Nano Lett 2010;10:1677–81.
[10] Zhou F, Wu S, Wu B, Chen WR, Xing D. Mitochondria-targeting single-walled carbon nanotubes for cancer photothermal therapy. Small 2011;7:2727–35.
[11] Barone PW, Strano MS. Reversible control of carbon nanotube aggregation for a glucose affinity sensor. Angew Chem Intl Ed 2006;45:8138–41.

[12] Anghileri LJ, Robert J. Hyperthermia in cancer treatment. Boca Raton, FL: CRC Press; 1986.
[13] Cho N, Cheong T, Min JH, Wu JH, Lee SJ, Kim D, et al. A multifunctional core-shell nanoparticle for dendritic cell-based cancer immunotherapy. Nat Nanotech 2011;6:675–82.
[14] Chen WR, Adams RL, Carubelli R, Nordquist RE. Laser-photosensitizer assisted immunotherapy: a novel modality in cancer treatment. Cancer Lett 1997;115:25–30.
[15] Chen WR, Singhal AK, Liu H, Nordquist RE. Laser immunotherapy induced antitumor immunity and its adoptive transfer. Cancer Res 2001;61:459–61.
[16] Garg AD, Nowis D, Golab J, Vandenabeele P, Krysko DV, Agostinis P. Immunogenic cell death, DAMPs and anticancer therapeutics: an emerging amalgamation. Biochim Biophys Acta 2010;1805:53–71.
[17] Zhou F, Xing D, Chen WR. Regulation of HSP70 on activating macrophages using PDT-induced apoptotic cells. Int J Cancer 2009;125:1380–9.